IEEE Access
Multidisciplinary | Rapid Review | Open Access Journal

Received August 22, 2019, accepted September 3, 2019, date of publication September 13, 2019,
date of current version September 30, 2019.

Digital Object Identifier 10.1109/ACCESS.2019.2941389

Iterative Clipping-Noise Compression Scheme for PAPR Reduction in OFDM Systems

BO TANG[1,2], KAIYU QIN[1,2], HAIBO MEI[1], AND CHANGWEI CHEN[1]
[1]School of Aeronautics and Astronautics, University of Electronic Science and Technology of China, Chengdu 611731, China
[2]Aircraft Swarm Intelligent Sensing and Cooperative Control Key Laboratory of Sichuan Province, Chengdu 611731, China

Corresponding author: Haibo Mei (haibo.mei@uestc.edu.cn)

ABSTRACT The application of orthogonal frequency division multiplexing (OFDM) has become more and more widespread in recent years. However, the high peak-to-average power ratio (PAPR) problem is still one of the critical issues in the implementation of OFDM systems. Among the techniques of PAPR reduction, iterative clipping and filtering (ICF) is widely used due to its easy implement, and many ICF-based methods have been proposed recently. The optimized ICF (OICF) further has been designed with an optimized filter and achieves faster convergence rate. And the simplified OICF (SOICF) applies Lagrange multiplier method to simplify the problem solving as compared to OICF. The approach saves SOICF from using complicated convex optimization methods. Most recently the clipping-noise compression (CNC) method is proposed to reduce the required number of Fourier transforms by compressing the clipping noise in the time domain. Based on SOICF, this paper adopts clipping and noise compression to replace the calculation of PAPR-reduction vector in each iteration. Analysis shows that the computational complexity of the proposed scheme is lower than SOICF. In addition, we have improved the CNC technique and introduced a compression threshold in the proposed scheme. In each iteration, only the components whose amplitude exceeds the compression threshold are compressed, while the others remain unchanged. To this end, this reduces the amount of information lost, resulting in better BER performance. The simulation results show that the proposed scheme has better BER performance than SOICF, and better PAPR reduction than CNC. When equal amounts of PAPR reduction by the evaluated methods are actually achieved, the BER performance of the proposed scheme is better than SOICF and CNC, especially with high-order modulation or lower clipping ratio.

INDEX TERMS Peak to average power ratio (PAPR), orthogonal frequency division multiplexing (OFDM), noise compression, computational complexity, iterative clipping and filtering (ICF).

I. INTRODUCTION

Due to the advantages including high spectral efficiency and strong resistance to multipath fading, orthogonal frequency division multiplexing (OFDM) has been widely adopted by many wireless communication standards such as IEEE 802.11, Digital Video Broadcasting (DVB), 4G and 5G mobile communications [1]–[6]. However, there are still some challenges on implementing OFDM in communication equipments. One of the major problems is the high peak-to-average power ratio (PAPR) of the transmitted OFDM signal, which requires a correspondingly large dynamic range of the transmitted signal path [7], [8]. In particular, as one of the main components consuming energy in the equipments, the power amplifier typically operates near its saturation region to achieve high efficiency, in which case high PAPR may result in nonlinear distortion [9]. Even though more power backoff can be taken to reduce the distortion, this however makes the amplifier inefficient [10], [11]. Therefore, it is necessary to study the PAPR reduction of OFDM signals [12].

To solve this issue, many techniques on PAPR reduction have been proposed in literatures. All these techniques can be categorized as distortionless-based methods and distortion-based methods [13]–[16]. The distortionless-based techniques including coding, multiple signaling and probabilistic, will not cause nonlinear distortion during PAPR reducing, but generally involve high

The associate editor coordinating the review of this manuscript and approving it for publication was Ivan Wang-Hei Ho.

computational complexity and side-information transmission [17], [18]. In contrast, the distortion-based techniques usually can be easily implemented and do not require side-information [19], [20].

Among these existing techniques, amplitude clipping and filtering is probably the simplest method of the distortion-based technologies [21]. It is achieved by limiting the peaks that exceed a predetermined threshold, which leads to in-band and out-of-band distortions. In order to meet the requirement of out-of-band radiation of the transmitted signal, a filter is usually required after clipping. But filtering will cause the peak regrowth. To address this problem, J. Armstrong proposed the iterative clipping and filtering (ICF) method in [22]. However, this method increases the computational complexity of the amplitude clipping and filtering technique.

The optimized iterative clipping and filtering (OICF) algorithm proposed by Wang and Luo in [23] can accelerate the convergence of iterations by replacing the rectangular filter with an optimized filter using convex optimization techniques. However, this method needs to solve the convex optimization problem, which is complicated. Zhu *et al.* proposed a simplified approach to OICF (SOICF) by studying clipping noise instead of clipped signals [24]. The SOICF technique reduces computational complexity by transforming convex optimization problems into the Lagrange multiplier method. Recently, some improved SOICF-based methods have been proposed. In [25], Anoh *et al.* applied an adaptive clipping threshold to SOICF to achieve faster convergence. Liu *et al.* proposed the enhanced ICF method which introduces the time-domain kernel matrix and the optimized corresponding scaling vector to generate the PAPR-reduction signal, and has been proved to more efficient than SOICF [26].

Wang and Tellambura proposed the simplified clipping and filtering technique (SCF) in [27], which requires only single iteration to achieve the same PAPR reduction as that of ICF. This thus reduces the number of fast Fourier transform (FFT) and inverse FFT (IFFT). However, since the clipping noise is scaled in the frequency domain, there are still three FFT/IFFTs required. And the computational complexity of FFT/IFFT will increase as the number of subcarriers increases. The neural network (NN) based SCF technique proposed by Sohn and Kim in [28] reduces the computational complexity by using only one IFFT module. However, in this approach, there are two additional NN modules based on multilayer perceptrons, and they need to be trained first. In addition, the performance of this method is also limited by its training samples. In [28], the SCF signals are used as training data, resulting that the PAPR reduction and bit error rate (BER) performance of the NN method could not be as good as SCF's. The clipping-noise compression (CNC) method is proposed in [29]. Since CNC carries out the processes all in the time domain, there is only one single Fourier transform needed. This reduces the computational complexity. And simulation results show that CNC also achieves better PAPR reduction and BER performance compared to the conventional ICF methods [29].

In this paper, our research focuses on the noise caused by clipping as SOICF and CNC. In SOICF, it is assumed that the phase of the clipping-noise peak is the same as that of its adjacent samples, and the suppression operations are applied to all the peaks and their adjacent samples. However, we found that as the clipping ratio decreases, the number of clipping noise peaks gradually increases. This makes the computational complexity increase and the BER performance degrade. Based on SOICF, we propose an iterative clipping-noise compression scheme for PAPR reduction. The proposed scheme uses the same clipping, clipping-noise calculation and iteration operations as SOICF. The difference is that the proposed scheme uses the noise compression technique to replace the PAPR reduction vector calculation, to reduce the computational complexity. In addition, the proposed scheme also improves the original CNC technique by introducing compression thresholds and iteration operations. Compared to CNC, the proposed scheme increases computational complexity, but it improves PAPR reduction and BER performance. When the same amounts of PAPR reduction are actually achieved, the proposed scheme has lower computational complexity and better BER performance compared to SOICF, especially in the case that the clipping ratio is low.

The remaining of the paper is organized as follows. In Section II, we introduce the background of the problem, including the system model of OFDM, and the involved previous works in the literatures. In Section III, the proposed iterative noise compression scheme is introduced, and the performance and computational complexity are analyzed. In Section IV, simulations are taken to evaluate the performance of the proposed scheme. Section V gives the conclusion.

II. SYSTEM MODEL AND PREVIOUS WORKS

In this section, we first introduce the OFDM system model and the PAPR problem in our study. Then, the involved methods proposed in the previous literatures, i.e., ICF, SOICF and CNC, are introduced and analyzed.

A. SYSTEM MODEL AND PAPR PROBLEM

OFDM is a commonly used multi-carrier modulation technique. And its wideband transmission can be considered as simultaneously transmitting several parallel narrowband signals. These narrowband signals named subcarriers are orthogonal to each other. In practice, the Fourier transforms are usually adopted to transform the OFDM signals from the frequency domain into the time domain to maintain the orthogonality of the subcarriers.

In practice, the signal is typically transmitted in a frame consisting of sequences of several time-domain OFDM symbols. In order to reduce interferences between symbols and conflicts with the multipath channels, cyclic prefix OFDM (CP-OFDM) is proposed and widely used [30]. Recently, based on CP-OFDM, some new post-OFDM waveforms have been proposed to smooth the transition between OFDM symbols, such as weighted overlap and add

based OFDM (WOLA-OFDM), filtered-OFDM (f-OFDM), filter-bank multi-carrier based on offset quadrature amplitude modulation (FBMC/OQAM) [31], [32]. However, these waveforms use IFFT on each OFDM symbol separately, resulting in their amplitude envelope characteristics similar in each symbol. Therefore, without loss of generality, the OFDM signal involved in this paper only works on a single OFDM symbol, as the works in [9]–[14].

The data to be transmitted should firstly be modulated by quadrature amplitude modulation (QAM) or phase shift keying (PSK), and then grouped as vectors with N components, and it is assumed that N is the number of the subcarriers in the OFDM systems. The vector is the OFDM symbol in the frequency domain, and can be described as

$$X_s = [X(0), X(1), \ldots, X(k), \ldots, X(N-1)], \tag{1}$$

where $X(k)$ is the k-th subcarrier of the OFDM symbol.

Moreover, oversampling is usually used in baseband processing to satisfy the Nyquist theorem and better approximate continuous signals. With L-time oversampling, X_s can be extended to with LN components by zero pading as

$$X = [X(0), X(1), \ldots, X(N-1), \underbrace{0, 0, \ldots, 0}_{(L-1)N}]. \tag{2}$$

The frequency-domain signal is usually transformed into the time domain using IFFT, so the discrete time-domain signal can be expressed as

$$x(n) = \frac{1}{\sqrt{LN}} \sum_{k=0}^{LN-1} X(k) e^{j\frac{2\pi nk}{LN}}, \tag{3}$$

where $x(n)$ is a complex signal that can be described as $x(n) = a(n) + jb(n)$, $a(n)$ is the real part and $b(n)$ is the imaginary part of $x(n)$, $X(k)$ are random variables of independent and identically distributed, due to the central limit theorem $a(n)$ and $b(n)$ being asymptotically independent and identical normal distributed variables [33]. Therefore, one gets that the magnitude $|x(n)| = \sqrt{(a(n)^2 + b(n)^2)}$ follows Rayleigh distribution [34]. That is, the peak power of $x(n)$ is usually much larger than the average power [35]. A widely used metric PAPR is proposed to describe the envelope characteristics of the signal, which is defined as

$$\mathrm{PAPR}[x(n)] = \frac{\max\limits_{0 \le n \le LN-1} [|x(n)|^2]}{\frac{1}{LN} \sum\limits_{n=0}^{LN-1} (|x(n)|^2)}. \tag{4}$$

Following (4), in order to evaluate the statistical properties of PAPR of OFDM symbols, the complementary cumulative distribution function (CCDF) is often used in PAPR reduction schemes [12], which is defined as

$$\mathrm{CCDF}[\mathrm{PAPR}(x(n))] = \mathrm{prob}[\mathrm{PAPR}(x(n)) > \mathrm{PAPR}_0], \tag{5}$$

where prob$[\cdot]$ is the probability operator and PAPR_0 is the reference threshold.

B. ITERATIVE CLIPPING AND FILTERING

In ICF, repeated clipping and filtering operations are ultilized to achieve the desired performance on PAPR reduction, while meeting the requirements of out-of-band radiation. The amplitudes of the signals over the predefined threshold are clipped, while the phases keep unchanged. This process is described as

$$\bar{x}(n) = \begin{cases} x(n), & |x(n)| \le A \\ Ae^{j\phi(n)}, & |x(n)| > A, \end{cases} \tag{6}$$

where $\bar{x}(n)$ denotes the clipped signal, A is the predefined clipping threshold, and $\phi(n)$ is the phase of $x(n)$. The threshold A is obtained by

$$A = \gamma \cdot \sqrt{P_{av}}, \tag{7}$$

where γ is clipping ratio and P_{av} is the average power of $x(n)$.

Since clipping is a non-linear process, it not only causes in-band distortion, but also leads to out-of-band power emission that is strictly limited in practical communication systems [9]. Thus, a process of filtering is required following the clipping. The classical ICF method proposed in [22] employs a rectangle filter, which is defined as

$$H(k) = \begin{cases} 1, & 0 \le k \le N-1 \\ 0, & N \le k \le LN-1, \end{cases} \tag{8}$$

where N equals to the number of OFDM subcarriers, and L denotes the oversampling factor.

According to (2), this filter removes the out-of-band components of the clipped signal while keeping the in-band components unchanged. The filtering improves spectral efficiency and BER performance, but it degrades the PAPR reduction due to the regrowth of peak. Therefore, the clipping and filtering processes should usually be repeated several times to achieve the expected PAPR reduction.

C. SIMPLIFIED APPROACH TO OPTIMIZED ITERATIVE CLIPPING AND FILTERING

In the ICF method, the filtering applies a rectangular filter, which simply eliminates the out-of-band components without considering the peak regrowth and in-band distortion. To optimize the filtering of each iteration in ICF, OICF therefore was proposed in [23]. In OICF, the rectangular filter is replaced by an optimized filter, which aims to minimize the error vector magnitude (EVM) of the current OFDM symbol subject to the desired PAPR.

The authors of [24] made an equivalent transformation of the optimization problem, and solved it by using the Lagrange multiplier method. SOICF proposes two algorithms with the same performance. In this paper, we take the algorithm using FFT as the implementation of SOICF because it has lower complexity according to [24]. Fig.1 shows the steps of the SOICF implementation.

Before the signal processing, in a OFDM system with N subcarriers and L time oversampling, the normalized basic

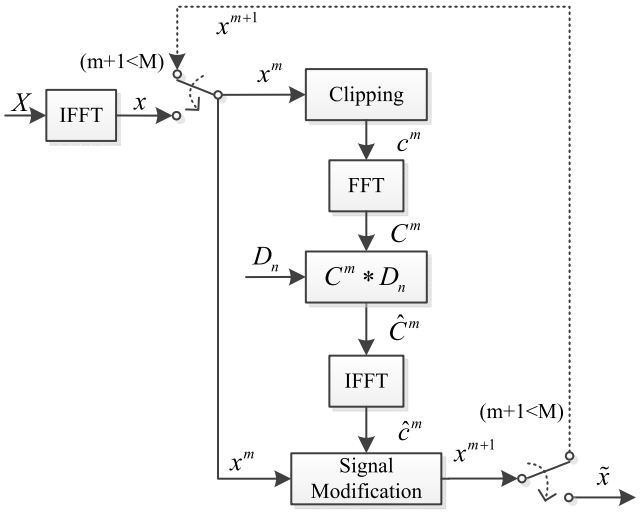

FIGURE 1. The implementation of SOICF.

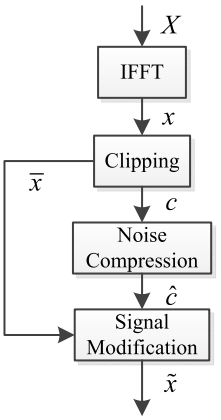

FIGURE 2. The implementation of CNC.

vector D_n needs to be calculated offline as follows

$$D_n = \frac{1}{\sqrt{N}}[\underbrace{1, 1, \ldots, 1}_{N}, \underbrace{0, 0, \ldots, 0}_{(L-1)N}]. \tag{9}$$

In addition, the clipping threshold A^m needs to be recalculated before the clipping of each iteration as $A^m = \gamma \cdot \sqrt{P_{av}^m}$, where the superscript m means the m-th iteration and the total number of iterations is M. It is assumed that P peaks when signal amplitude exceeds A^m, and they are clipped respectively to obtain the cliping-noise signal c^m, which is calculated as

$$c^m(n_p) = (|x^m(n_p)| - A^m)e^{j\phi^m(n_p)}. \tag{10}$$

where it is assumed that the peak occurs at n_p and there are P peaks exceeding the threshold.

The next step is to use FFT to transform c^m into the frequency domain to obtain $C^m = \text{FFT}(c^m)$. Then the PAPR-reduction vector $\hat{C}^m$ in the frequency domain can be calculated as

$$\hat{C}^m = C^m D_n. \tag{11}$$

Then, an IFFT is used to transform $\hat{C}^m$ into the time domain to get $\hat{c}^m = \text{IFFT}(\hat{C}^m)$, and the PAPR reduced signal is calculated as

$$x^{m+1} = x^m - \hat{c}^m. \tag{12}$$

When m is less than the number of iterations M, clipping and PAPR-reduction vector calculating are repeated. Otherwise, x^{m+1} is transmitted as the output signal $\tilde{x}$.

Overall, we can see that SOICF being an improved method based on ICF and OICF, it replaces the solution of the optimized filter problem in OICF with a simplified method. To this end, the computational complexity of SOICF is reduced compared to OICF. However, SOICF introduces a pair of Fourier transforms during the calculation of the PAPR-reduction vector in each iteration. And this also leads to a high computational complexity due to the FFT, which increases as the clipping ratio decreases because more peaks are clipped. Therefore, we consider to replace the calculation of PAPR-reduction vector with a more simplified and effective method, which is introduced in the next section.

D. CLIPPING-NOISE COMPRESSION

Similar to SOICF, CNC also focus on clipping noise instead of clipped signals. To reduce the number of FFT/IFFTs, noise compression and signal modification are performed in the time domain.

The implementation of CNC is shown as Fig.2. Firstly, an IFFT is used to transform the frequency-domain signal to the time-domain signal x. And x is clipped according to (6). Then, the clipping-noise is calculated as

$$c(n) = x(n) - \bar{x}(n). \tag{13}$$

Then, the compressed noise can be calculated as

$$\hat{c}(n) = \frac{\text{E}[|c(n)|]\ln[1 + \mu \frac{|c(n)|}{\text{E}[|c(n)|]}]}{\ln(1+\mu)} e^{j\phi_c(n)}, \tag{14}$$

where $\text{E}[\cdot]$ denotes the expectation operation, μ is the compression factor, and $\phi_c(n)$ is the phase of $c(n)$.

Finally, the desired transmitted signal is obtained as

$$\tilde{x}(n) = \bar{x}(n) + \hat{c}(n). \tag{15}$$

The CNC method reduces the computational complexity, and the simulation results show that it improves the PAPR reduction and BER performance compared to the conventional ICF based methods [29]. However, the CNC method directly compresses all signal amplitudes that exceed the clipping threshold. This indiscriminate one-time compression method also compresses some amplitudes, which do not affect the peak of the transmitted signal even if they are not compressed. This leads to a drop in BER performance. Therefore, we consider to introduce the compression threshold and adopt iterative operations in our proposed scheme.

III. THE PROPOSED SCHEME AND THE ANALYSIS

Compared to SOICF and CNC, in this paper we propose a new method called iterative noise compression scheme for PAPR reduction. In this section, the description and analysis of the proposed scheme are presented, followed by an analysis of the computational complexity.

A. DESCRIPTION OF THE PROPOSED SCHEME

According to the analysis in the last section, we consider combining SOICF and CNC to obtain a new solution for better performance. By comparing Fig.1 and Fig.2, we can see that the clipping and the clipping-noise calculation of CNC are the same as that of SOICF. And the modules of signal modification are almost the same, except for that the signal x^m adopted in SOICF is pre-clipping, while $\overline{x}$ used in CNC is post-clipping. Therefore, we consider applying the module of noise compression in CNC to replace the module of PAPR reduction vector calculation in SOICF, i.e., the modules of FFT/IFFT and the frequency-domain vector $\hat{C}^m$ calculation. Furthermore, the iterative operation in SOICF is inherited and the noise compression technique is improved. The proposed scheme can be described as follows.

We update the clipping ratio for each iteration as

$$\gamma^m = \gamma + \frac{(M-m)\cdot\gamma}{M}, \tag{16}$$

where γ^m is the clipping ratio of the m-th iteration, and M is the total number of iterations. Equation (16) shows that as m increases, the clipping ratio γ^m gradually decreases. The value of clipping ratio γ^M in the last iteration is equal to the preset value γ to achieve the desired PAPR reduction.

In addition, we can see that the PAPR in (4) is determined by the maximum and the average power of the signal. Since the amplitude of the OFDM signal follows the Rayleigh distribution [35], there are fewer components with amplitude exceeding the clipping threshold, resulting in little effect on the average power of the signal. Therefore, in CNC, the maximum amplitude of the compressed noise has a critical effect on the PAPR performance.

The characteristics of the μ-law compression algorithm show that it is a monotonic function [29]. That is to say, the maximum amplitude of the compressed signal is determined by the maximum amplitude of the signal before compression. Therefore, we consider keeping the clipping-noise components whose amplitudes below the compressed maximum peak unchanged. This would not degrade the performance of PAPR reduction, but improves the BER performance as the number of compressed noise components decrease.

Specifically, before the noise compression process, we firstly find the component $c(n_{\max})$ with the largest amplitude in the clipping noise $c(n)$ obtained by (13), and then calculate its compressed signal $\hat{c}(n_{\max})$ as follows

$$\hat{c}(n_{\max}) = \frac{\alpha \ln(1+\mu\frac{|c(n_{\max})|}{\alpha})}{\ln(1+\mu)} e^{j\phi_c(n_{\max})}, \tag{17}$$

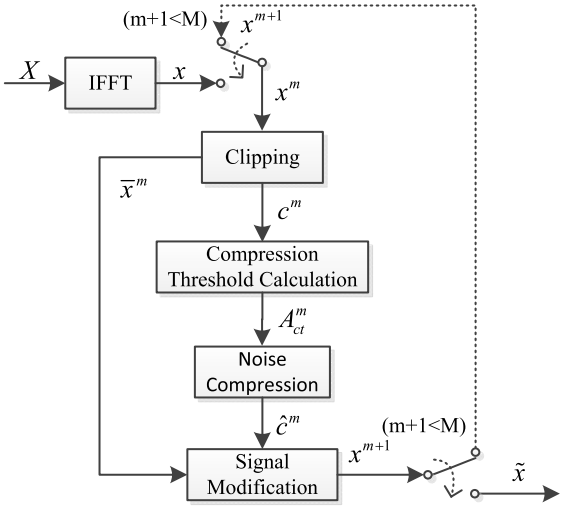

FIGURE 3. The implementation of the proposed scheme.

where μ is the compression factor, α is the normalization factor, which is calculated by $\alpha = \mathrm{E}[c(n)]$, and $\phi_c(n_{\max})$ is the phase of $c(n_{\max})$.

According to the previous analysis, in CNC, $\hat{c}(n_{\max})$ is with the maximum amplitude of the compressed noise, which almost determines the PAPR of the transmitted signal. Therefore, in our study, the amplitude of $\hat{c}(n_{\max})$ is taken as the compression threshold

$$A_{ct} = |\hat{c}(n_{\max})|. \tag{18}$$

Then, the process of noise compression is described as follows

$$\hat{c}(n) = \begin{cases} c(n), & |c(n)| \le A_{ct} \\ \dfrac{\alpha \ln(1+\mu\frac{|c(n)|}{\alpha})}{\ln(1+\mu)} e^{j\phi_c(n)}, & |c(n)| > A_{ct}, \end{cases} \tag{19}$$

where $\hat{c}(n)$ is the compressed noise, and $\phi_c(n)$ is the phase of $c(n)$. As shown in (19), in the proposed compression algorithm, $c(n)$ is compressed only when $|cn| > A_{ct}$, otherwise remains unchanged. And, A_{ct} is calculated according to (17) and (18), which equals to the peak amplitude of the compressed noise obtained by using CNC.

In summary, the implementation of the proposed scheme is shown in Fig.3. The specific steps are as follows.

1) Use IFFT to obtain the time-domain OFDM signal x. It is assumed that the total number of iteration is M, and the superscript m denotes m-th iteration. Set $m = 1$, and let $x^m = x$ be used as the input for the first clipping.
2) Calculate the clipping threshold A^m of the OFDM signal as $A^m = \gamma^m \cdot \sqrt{P_{av}^m}$, where γ^m is calculated according to (16), and P_{av}^m is the average power of x^m.
3) Clip x^m and obtain $\overline{x}^m$ as

$$\overline{x}^m(n) = \begin{cases} x^m(n), & |x^m(n)| \le A^m \\ A^m e^{j\phi^m(n)}, & |x^m(n)| > A^m, \end{cases} \tag{20}$$

where $\phi^m(n)$ is the phase of $x^m(n)$.

4) Calculate the clipping-noise as

$$c^m(n) = x^m(n) - \bar{x}^m(n). \tag{21}$$

5) Find the component with the largest amplitude in the clipping noise, and calculate its compressed signal. The compression threshold can be obtained as

$$A_{ct}^m = \frac{\alpha \ln(1 + \mu \frac{|c^m(n_{\max})|}{\alpha})}{\ln(1+\mu)}, \tag{22}$$

where μ is the compression factor, α is calculated by $\alpha = \mathrm{E}[c^m(n)]$, and $c^m(n_{\max})$ is with the largest amplitude of $c^m(n)$.

6) The components with amplitudes greater than the compression threshold A_{ct}^m are compressed, and the others keep unchanged, as follows

$$\hat{c}^m(n) = \begin{cases} c^m(n), & |c^m(n)| \le A_{ct}^m \\ \dfrac{\alpha \ln(1 + \mu \frac{|c^m(n)|}{\alpha})}{\ln(1+\mu)} e^{j\phi_c^m(n)}, & |c^m(n)| > A_{ct}^m, \end{cases} \tag{23}$$

where $\phi_c^m(n)$ is the phase of $c^m(n)$.

7) Modify the clipped signal as

$$x^{m+1}(n) = \bar{x}^m(n) + \hat{c}^m(n). \tag{24}$$

8) If $m < M$, set $m = m + 1$ and repeat Steps 2)-7). Otherwise, output x^{m+1} as the transmitted signal $\widetilde{x}$.

B. ANALYSIS OF THE PROPOSED SCHEME

In this subsection, we first analyze the PAPR reduction of the proposed scheme compared with CNC, as well as the BER performance via EVM analysis. Then, we give the analysis of BER performance of the proposed scheme comparing to SOICF with lower clipping ratio.

The proposed scheme adopts an iterative approach by which PAPR is reduced during each iteration. At the last iteration, the clipping ratio equals to the predefined threshold, while the signal's PAPR is smaller than the original signal due to the performed iterations. This leads to a lower peak amplitude, resulting in a better PAPR reduction for this scheme than CNC.

In each iteration of the proposed scheme, the compression threshold A_{ct}^m is calculated before noise compression. The threshold is defined as the maximum amplitude of the compressed noise signal. According to (20),(23) and (24), the largest amplitude of x^{m+1} depends on the compression threshold, which is equals to the largest amplitude obtained by CNC. That is to say, the proposed scheme introduces a compression threshold, and does not change the peak power of the modified signal. According to (23), the noise components with amplitude below A_{ct}^m are not compressed, resulting in the average power of the modified signal being larger than that of the CNC. According to the definition of PAPR, when the peak power of the signal keeps the same, the larger the average power, the smaller the PAPR. Therefore, even with one iteration, the proposed scheme has better PAPR reduction than CNC.

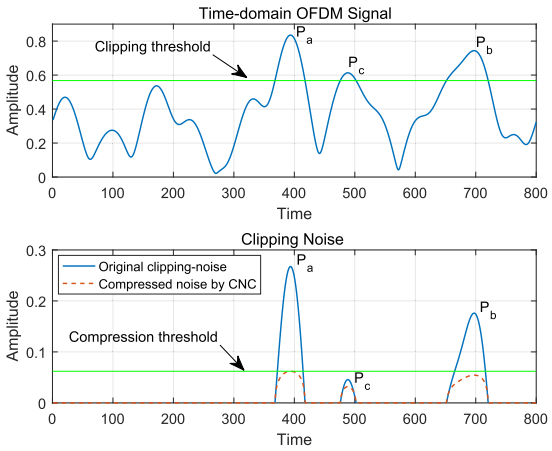

FIGURE 4. An example of the process of clipping and noise compression.

An example of the process of clipping and noise compression is shown as in Fig.4. We can see in the upper subfigure that there are three peaks exceeding the clipping threshold, and P_a is with the largest amplitude. Then, the compressed peak $\hat{P}_a$ is used as the compression threshold A_{ct}. From the bottom subfigure of Fig.4, we can see that P_b is larger and P_c is smaller than A_{ct}. All the three peaks are compressed in CNC, while only P_a and P_b are compressed in the proposed scheme. It can be seen that in both methods the largest peak power of the compressed signal is determined by $\hat{P}_a$, while the averge power of the proposed scheme is higher because the peak P_c is kept uncompressed. This leads to better PAPR reduction and BER performance.

EVM is a commonly used metric for signal distortion and it can be applied in the analysis of BER performance [23]. It is defined as

$$\mathrm{EVM} = \frac{||X - \widetilde{X}||_2}{||X||_2}, \tag{25}$$

where X is the original frequency-domain OFDM signal, and $\widetilde{X}$ is the frequency-domain signal with PAPR reduced. By using the Parseval's theorem, we can rewrite the numerator of (25) as

$$||X - \widetilde{X}||_2 = LN||x - \widetilde{x}||_2. \tag{26}$$

where it can be seen that the difference between the original and the modified signals is proportional to EVM. According to the previous analysis, in the proposed scheme, only components whose amplitude exceeding the threshold are compressed. That is to say, compared to CNC, the proposed scheme compresses fewer components of the clipping noise and thus has better EVM performance.

In SOICF, it is assumed that the peak and its adjacent samples have the same phase. However, when the clipping ratio is lowered, a clipping segment lasts longer and the

phase difference is not sufficiently small. In addition, as lower clipping ratio, the number of clipping segments increases. Since the PAPR reduction vector calculation involves not only the peak but also its adjacent samples, when the number of clipping segments increases, some samples may be excessively suppressed, resulting in a decrease in BER performance. Unlike SOICF, the proposed scheme only compresses samples whose amplitude exceeds the compression threshold, while the other samples remain unchanged. This allows for a lower total amount of information lost during signal processing, leading to better BER performance.

In summary, the above analysis shows that the proposed scheme has better PAPR reduction and BER performance than CNC, and better BER performance than SOICF when lower clipping ratio adopted. This conclusion will be verified by simulation in the next section.

C. COMPLEXITY ANALYSIS

As the computational complexity depends on the number of subcarriers of OFDM symbols, the big-Oh notation is used for complexity analysis [23].

ICF requires a pair of FFT/IFFTs with $O(2LN\log_2(LN))$ complexity for each iteration [36]. The complexity required for A^m calculation and clipping is $O(2LN)$. To convert the signal from the frequency domain to the time domain before the first iteration, an additional IFFT is required. Therefore, the total complexity of the ICF for M iterations is $O((2M+1)LN\log_2(LN)+2MLN)$.

In SOICF, the complexity required for A^m calculations and clipping is $O(2LN)$ in each iteration. To calculate the frequency-domain PAPR-reduction vector $\hat{C}^m$ in (11), the complexity is $O(LN)$. An pair of FFT/IFFTs results in $O(2LN\log_2(LN))$ complexity. The calculation of x^{m+1} in (12) requires $O(LN)$. Therefore, the complexity required for each iteration is $O(2LN\log_2(LN)+4LN)$, and the total complexity of M iterations is $O((2M+1)LN\log_2(LN)+4MLN)$.

In CNC, the number of FFT/IFFTs required is one, resulting in the complexity of $O(LN\log_2(LN))$. The clipping requires $O(2LN)$ complexity, and the compression in (14) requires the complexity of $O(2LN)$. Since the algorithm does not require iteration, its total complexity is $O(LN\log_2(LN)+4LN)$.

In the proposed scheme, only one IFFT is needed to transform the OFDM signal from the frequency domain to the time domain, resulting in the complexity of $O(LN\log_2(LN))$. The same as that in CNC, the clipping and compression process requires $O(4LN)$ complexity in each iteration. In addition, (22) requires $O(LN)$ complexity due to the need to calculate the noise compression threshold. Therefore, the total complexity required for M iterations is $O(LN\log_2(LN)+5MLN)$.

The computational complexity comparison of the evaluated schemes is shown in Table.1. We can see that CNC has the smallest algorithm complexity. The complexity of the proposed method is higher than that of CNC, but lower than that of other schemes.

TABLE 1. Computational complexity comparison.

Scheme	Computational complexity
ICF	$O((2M+1)LN\log_2(LN)+2MLN)$
SOICF	$O((2M+1)LN\log_2(LN)+4MLN)$
CNC	$O(LN\log_2(LN)+4LN)$
The proposed scheme	$O(LN\log_2(LN)+5MLN)$

IV. SIMULATION RESULTS

In this section, we firstly evaluated the PAPR reduction and BER performance of the proposed scheme, with clipping ratio high, medium, and low, respectively. Then, we took the evaluation of the out-of-band radiation. At last, we carefully adjusted the clipping ratios of the evaluated methods respectively so that they have the same amount of PAPR reduction. In this case, we evaluated the BER performance like [24].

A. PAPR REDUCTION AND BER PERFORMANCE EVALUATION

In the simulations, number of the subcarriers is set to $N = 128$, and the modulation of the subcarriers is quadrature phase shift keying (QPSK) in the OFDM system. The oversampling factor is set to $L = 4$. The number of iterations is set to $M = 3$ for the schemes requiring iteration. The compression factor μ is set to 3 for CNC and the proposed scheme.

The simulations were taken to evaluate the PAPR reduction of the evaluated schemes with a specific clipping ratio, and the BER performance with the signals through an additive white Gaussian noise (AWGN) channel. Without loss of generality, γ is set to 2.1, 1.8, and 1.5 as high, medium, and low clipping ratios respectively in the simulations.

Fig.5 shows the CCDF and BER curves of the evaluated signals with $\gamma = 2.1$. It can be seen from the figure that compared with the unclipped signal, all the PAPR-reduced signals have obvious reduction of PAPRs, and their BER curves are all close to the unclipped signal's curve. This is mainly because the higher clipping ratio causes the fewer number of peaks clipped, resulting in lower total amount of information lost. Specifically, among the schemes, SOICF has the best PAPR reduction, but also has the worst BER performance. The PAPR reduction of the CNC and the proposed scheme is better than that of ICF. The BER performance of the proposed scheme and CNC is very similar, while the PAPR reduction of the proposed scheme is better than that of the CNC.

Fig.6 shows the CCDF and BER curves of the transmitted signal with $\gamma = 1.8$. We can see that, as the clipping ratio decreases, the PAPR reduction of the signals in all schemes are improved, while the BER performances become worse. As can be seen from the figure, the SOICF signal has the lowest PAPRs and the worst BER performance. The ICF's PAPR reduction and BER performance are worse than that of the CNC and the proposed scheme. As can be seen from Fig.6-(b), the proposed scheme and CNC have similar

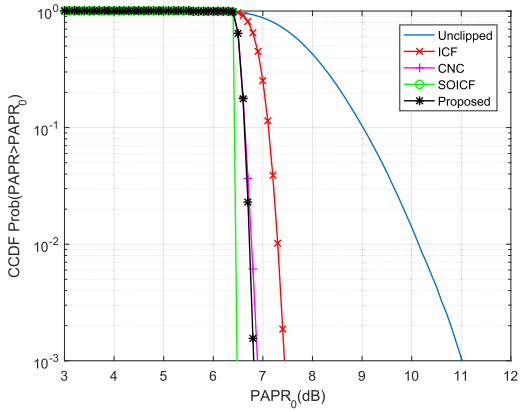

(a) The PAPR reduction comparison of the evaluated methods with $\gamma = 2.1$.

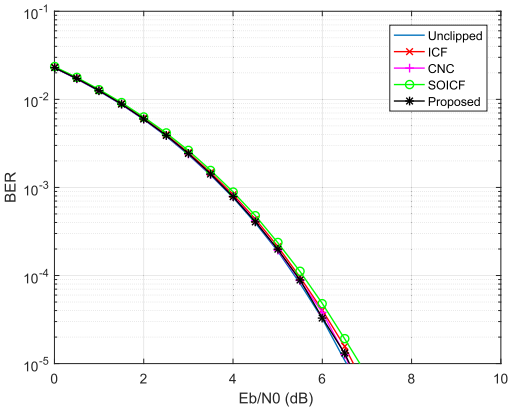

(b) The BER performance comparison of the evaluated methods with $\gamma = 2.1$.

FIGURE 5. The CCDF and BER curves of the evaluated signals with QPSK, $\gamma = 2.1$.

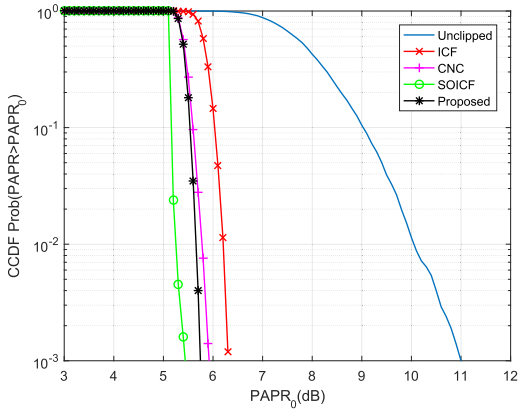

(a) The PAPR reduction comparison of the evaluated methods with $\gamma = 1.8$.

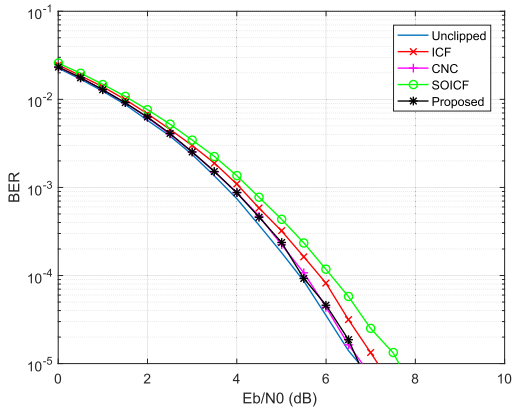

(b) The BER performance comparison of the evaluated methods with $\gamma = 1.8$.

FIGURE 6. The CCDF and BER curves of the evaluated signals with QPSK, $\gamma = 1.8$.

BER performance, which is better than SOICF and ICF. At the same time, according to Fig.6-(a), the proposed scheme has a better PAPR reduction compared to CNC at the CCDF probability of 10^{-3}.

Fig.7 shows the CCDF and BER curves of the transmitted signals with $\gamma = 1.5$. We can see that the smaller clipping ratio leads to the PAPR reduction of the evaluated schemes more obvious, and the BER performance difference becomes larger. Specifically, as can be seen from Fig.7-(b), the BER performances of the proposed scheme and CNC are very similar, and significantly better than that of ICF and SOICF (at a BER of 10^{-5}, about 2dB better than ICF, and more than 3dB better than SOICF). Furthermore, as can be seen from Fig.7-(a), at a CCDF probability of 10^{-3}, the PAPR reduction of the proposed scheme is about 0.4dB better than that of the other schemes.

The simulation results show that with a specific clipping ratio, SOICF has acceptable BER performance and better PAPR reduction when γ is larger, while the proposed scheme also has significant PAPR reduction and BER performance. When γ is small, the PAPR reduction and BER performance of the proposed schemes are better than that of the other schemes.

B. OUT-OF-BAND RADIATION EVALUATION

The PAPR-reduced signals are passed through a solid-state power amplifier (SSPA) to evaluate the out-of-band radiation performance. The commonly used AM/AM conversion of SSPA model is adopted in the simulations [37]. The input and output signal of the model can be given as

$$s_{out}(t) = \frac{|s_{in}(t)|}{(1 + (\frac{|s_{in}(t)|}{s})^{2p})^{1/2p}} e^{j\phi(t)}, \tag{27}$$

where $s_{in}(t)$ and $s_{out}(t)$ are respectively the input and output signals of the SSPA, and $\phi(t)$ is the phase of $s_{in}(t)$. The parameter s indicates the input saturation level and p indicates the AM/AM sharpness [37]. We set s to 2.4 and p to 3 in the simulations. The power spectral densities of the PAPR-reduced signals with $\gamma = 1.8$ are shown in Fig.8.

As can be seen that all the evaluated PAPR reduction schemes have significantly improved the out-of-band nonlinear distortion of the amplifier. Among them, SOICF has the lowest out-of-band radiation distortion, and the proposed scheme has similar performance as CNC.

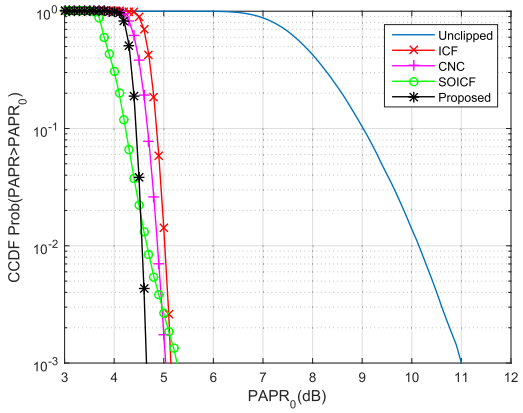

(a) The PAPR reduction comparison of the evaluated methods with $\gamma = 1.5$.

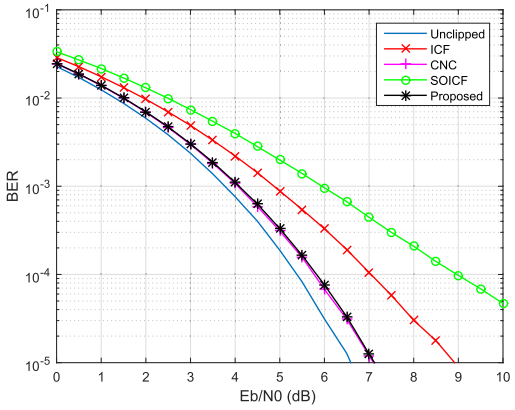

(b) The BER performance comparison of the evaluated methods with $\gamma = 1.5$.

FIGURE 7. The CCDF and BER curve of the compressed signal with QPSK, $\gamma = 1.5$.

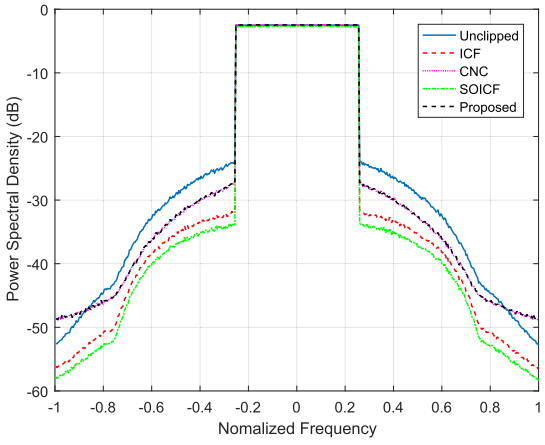

FIGURE 8. Out-of-band radiation comparison of OFDM signals.

C. BER PERFORMANCE WITH SIMILAR PAPRS ACTUALLY ACHIEVED

Since the clipping ratio indicates the desired PAPR performance, the actually achieved PAPR performance depends on the method used. Here the simulations were taken to compare

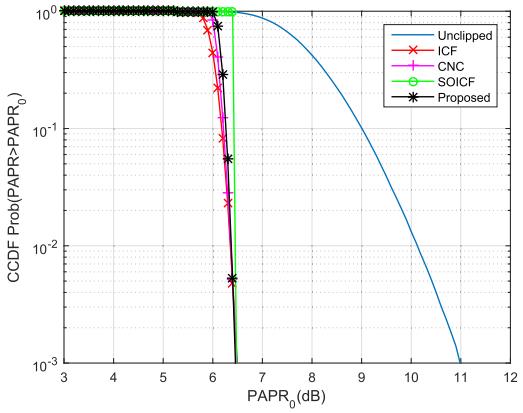

(a) The CCDF curves of ICF, CNC, SOICF, and the proposed scheme with γ=1.84, 1.98, 2.1, 2, respectively.

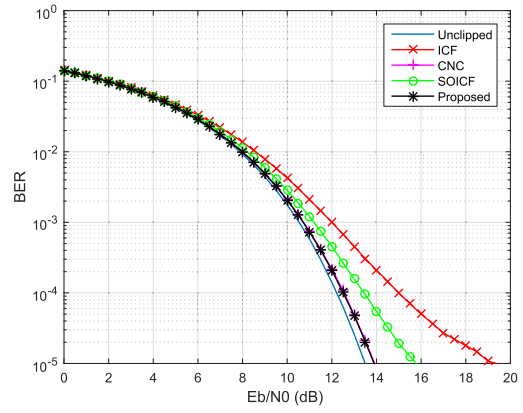

(b) The BER performance comparison of ICF, CNC, SOICF, and the proposed scheme with γ=1.84, 1.98, 2.1, 2, respectively.

FIGURE 9. The CCDF and BER curves of the evaluated signals with 16QAM and higher γ when similar actually PAPRs achieved.

the BER performance of the proposed method and other schemes in the case that the actually equal amounts of PAPR reduction are achieved.

We consider an OFDM system with 16QAM modulation and 128 subcarriers. The oversampling factor L is set to 4. The number of iterations is set to 3 (if needed). The compression factor is set to 3 for CNC and the proposed scheme.

First, we set a fixed clipping ratio γ for the proposed scheme, and take simulations to obtain the actually achieved PAPRs. Then, we carefully adjust the values of γ for the other schemes untill they achieves the same PAPRs that obtained using the proposed method. Finally, we compare the BER performance of the methods with an AWGN channel when the same PAPRs actually achieved.

Fig.9 compares the BER performance of the evaluated methods. The clipping ratio γ is set to 1.84, 1.98, 2.1, 2 for ICF, CNC, SOICF and proposed scheme, respectively. Their CCDF curves are shown in Fig.9-(a), and it can been seen that they have similar PAPR performance when the CCDF is 10^{-3}. Fig.9-(b) shows their BER comparison. It can be seen

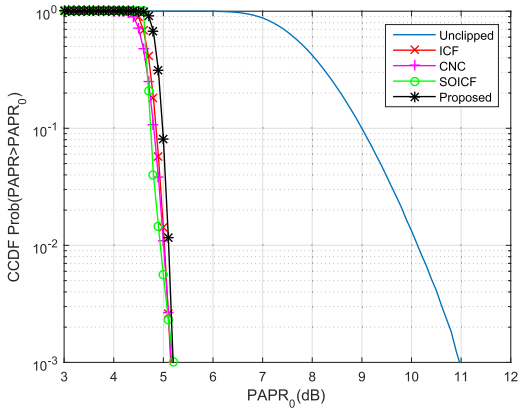

(a) The CCDF curves of ICF, CNC, SOICF, and the proposed scheme with γ=1.5, 1.55, 1.7, 1.6, respectively.

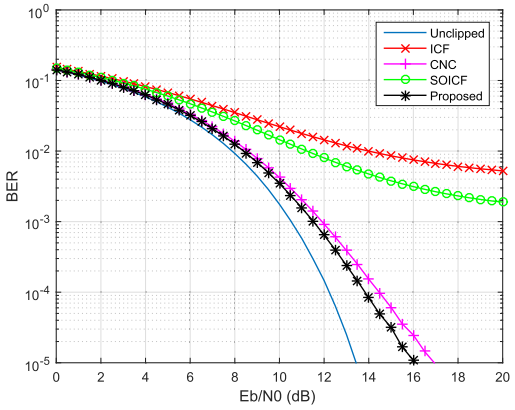

(b) The BER performance comparison of ICF, CNC, SOICF, and the proposed scheme with γ=1.5, 1.55, 1.7, 1.6, respectively.

FIGURE 10. The CCDF and BER curves of the evaluated signals with 16QAM and lower γ when similar actually PAPRs achieved.

from the figure that the BER of SOICF is better than ICF, and the BER performance of the proposed scheme and CNC is similar. When the BER is 10^{-5}, the required signal to noise ratio (SNR) of the proposed scheme is about 5dB better than ICF, and about 2dB better than SOICF.

Fig.10 compares the BER performance of the evaluated methods. The clipping ratio γ is set to 1.5, 1.55, 1.7, 1.6 for ICF, CNC, SOICF and the proposed scheme, respectively. Their CCDF curves are shown in Fig.10-(a), and it can been seen that they have similar PAPR performance when the CCDF is 10^{-3}. Fig.10-(b) shows their BER comparison. It can be seen from the figure that the BER performance of the proposed scheme and CNC are significantly better than that of SOICF and ICF. And furthermore, when the BER is 10^{-5}, the required SNR of the proposed scheme is about 1dB better than CNC.

The simulation results show that the proposed scheme and CNC provide better BER performance than ICF and SOICF when similar PAPRs is actually achieved. Furthermore, the BER performance of the proposed scheme is better than the case of CNC, especially when clipping ratio γ is small.

In addition, the simulations of this subsection adopts 16QAM instead of the QPSK used in Subsection A of this section. According to the comparison of Fig.5-(b) and Fig.9-(b), and the comparison of Fig.7-(b) and Fig.10-(b), it can be found that as the modulation order increases, the BER performance of ICF and SOICF degrades dramatically, while the BER performance of CNC and the proposed scheme changes smoothly. When clipping ratio γ is low, the BER performance of the proposed scheme is significantly better than the other evaluated methods.

Therefore, we can conclude that the proposed scheme has better BER performance than SOICF, and better PAPR reduction than CNC. Both PAPR reduction and BER performance of the proposed scheme are better than the case of ICF. When equal amounts of PAPR reduction are actually achieved, the BER performance of the proposed scheme is better than that of the other evaluated methods, especially with high-order modulation or lower clipping ratio.

V. CONCLUSION

In this paper, we firstly investigated two clipping based methods of PAPR reduction – SOICF and CNC. Then, we proposed the new scheme by using the clipping-noise compression technique in CNC to replace the PAPR-reduction vector calculation in SOICF. In addition, we have improved the clipping-noise compression technique in the proposed scheme by introducing a compression threshold. Analysis shows that the computational complexity of the proposed scheme is lower than that of SOICF. Compared to CNC, the proposed scheme has higher computational complexity, but improves the PAPR reduction and BER performance. At the end, we have carried out simulations to evaluate the performance of the proposed scheme. Simulation results show that the proposed scheme has better BER performance than SOICF, and better PAPR reduction than CNC. When equal amounts of PAPR reduction are actually achieved, the BER performance of the proposed scheme is better than SOICF and CNC, especially with high-order modulation or lower clipping ratio.

In future work, we intend to apply the proposed scheme to different OFDM systems with particular waveforms for PAPR reduction. In addition, we plan to combine the proposed scheme with the distortionless methods, such as coding, multiple signaling & probabilistic techniques, etc., to form a hybrid technology having more advantages.

REFERENCES

[1] T. Hwang, C. Yang, G. Wu, S. Li, and G. Y. Li, "OFDM and its wireless applications: A survey," *IEEE Trans. Veh. Technol.*, vol. 58, no. 4, pp. 1673–1694, May 2009.

[2] S.-Y. Lien, S.-L. Shieh, Y. Huang, B. Su, Y.-L. Hsu, and H.-Y. Wei, "5G new radio: Waveform, frame structure, multiple access, and initial access," *IEEE Commun. Mag.*, vol. 55, no. 6, pp. 64–71, Jun. 2017.
[3] L. Dai, Z. Wang, and Z. Yang, "Next-generation digital television terrestrial broadcasting systems: Key technologies and research trends," *IEEE Commun. Mag.*, vol. 50, no. 6, pp. 150–158, Jun. 2012.
[4] I. Eizmendi, M. Velez, D. Gómez-Barquero, J. Morgade, V. Baena-Lecuyer, M. Slimani, and J. Zoellner, "DVB-T2: The second generation of terrestrial digital video broadcasting system," *IEEE Trans. Broadcast.*, vol. 60, no. 2, pp. 258–271, Jun. 2014.
[5] E. Khorov, A. Kiryanov, A. Lyakhov, and G. Bianchi, "A tutorial on IEEE 802.11 ax high efficiency WLANs," *IEEE Commun. Surveys Tuts.*, vol. 21, no. 1, pp. 197–216, 1st Quart., 2019.
[6] J. Kim and I. Lee, "802.11 WLAN: History and new enabling MIMO techniques for next generation standards," *IEEE Commun. Mag.*, vol. 53, no. 3, pp. 134–140, Mar. 2015.
[7] G. Wunder, R. F. H. Fischer, H. Boche, S. Litsyn, and J.-S. No, "The PAPR problem in OFDM transmission: New directions for a long-lasting problem," *IEEE Signal. Process. Mag.*, vol. 30, no. 6, pp. 130–144, Nov. 2013.
[8] D. Chen, Y. Tian, D. M. Qu, and T. Jiang, "OQAM-OFDM for wireless communications in future Internet of Things: A survey on key technologies and challenges," *IEEE Internet Things J.*, vol. 5, no. 5, pp. 3788–3809, Oct. 2018.
[9] D. Feng, C. Jiang, G. Lim, L. J. Cimini, Jr., G. Feng, and G. Y. Li, "A survey of energy-efficient wireless communications," *IEEE Commun. Surveys Tuts.*, vol. 15, no. 1, pp. 167–178, 1st Quart., 2013.
[10] P. M. Lavrador, T. R. Cunha, P. M. Cabral, and J. C. Pedro, "The linearity-efficiency compromise," *IEEE Microw. Mag.*, vol. 11, no. 5, pp. 44–58, Aug. 2010.
[11] F. Sandoval, G. Poitau, and F. Gagnon, "Hybrid peak-to-average power ratio reduction techniques: Review and performance comparison," *IEEE Access*, vol. 5, pp. 27145–27161, 2017.
[12] T. Jiang and Y. Wu, "An overview: Peak-to-average power ratio reduction techniques for OFDM signals," *IEEE Trans. Broadcast.*, vol. 54, no. 2, pp. 257–268, Jun. 2008.
[13] J. Joung, C. K. Ho, K. Adachi, and S. Sun, "A survey on power-amplifier-centric techniques for spectrum- and energy-efficient wireless communications," *IEEE Commun. Surveys Tuts.*, vol. 17, no. 1, pp. 315–333, 1st Quart., 2015.
[14] Y. Rahmatallah and S. Mohan, "Peak-to-average power ratio reduction in OFDM systems: A survey and taxonomy," *IEEE Commun. Surveys Tuts.*, vol. 15, no. 4, pp. 1567–1592, 4th Quart., 2013.
[15] Y. A. Jawhar, L. Audah, M. A. Taher, K. N. Ramli, N. S. M. Shah, M. Musa, and M. S. Ahmed, "A review of partial transmit sequence for PAPR reduction in the OFDM systems," *IEEE Access*, vol. 7, no. 1, pp. 18021–18041, Feb. 2019.
[16] A. M. Rateb and M. Labana, "An optimal low complexity PAPR reduction technique for next generation OFDM systems," *IEEE Access*, vol. 7, pp. 16406–16420, 2019.
[17] K. G. Paterson and V. Tarokh, "On the existence and construction of good codes with low peak-to-average power ratios," *IEEE Trans. Inf. Theory*, vol. 46, no. 6, pp. 1974–1987, Sep. 2000.
[18] R. W. Bäuml, R. F. H. Fischer, and J. B. Huber, "Reducing the peak-to-average power ratio of multicarrier modulation by selected mapping," *Electron. Lett.*, vol. 32, no. 22, pp. 2056–2057, Oct. 1996.
[19] X. Li and L. J. Cimini, "Effects of clipping and filtering on the performance of OFDM," *IEEE Commun. Lett.*, vol. 2, no. 5, pp. 131–133, May 1998.
[20] X. Huang, J. Lu, J. Zheng, J. Chuang, and J. Gu, "Reduction of peak-to-average power ratio of OFDM signals with companding transform," *Electron. Lett.*, vol. 37, no. 12, pp. 506–507, Apr. 2001.
[21] S.-P. Lin, Y.-F. Chen, and S.-M. Tseng, "Iterative smoothing filtering schemes by using clipping noise-assisted signals for PAPR reduction in OFDM-based carrier aggregation systems," *IET Commun.*, vol. 13, no. 6 pp. 802–808, Apr. 2019.
[22] J. Armstrong, "Peak-to-average power reduction for OFDM by repeated clipping and frequency domain filtering," *Electron. Lett.*, vol. 38, no. 5, pp. 246–247, Feb. 2002.
[23] Y.-C. Wang and Z.-Q. Luo, "Optimized iterative clipping and filtering for PAPR reduction of OFDM signals," *IEEE Trans. Commun.*, vol. 59, no. 1, pp. 33–37, Jan. 2011.
[24] X. Zhu, W. Pan, H. Li, and Y. Tang, "Simplified approach to optimized iterative clipping and filtering for PAPR reduction of OFDM signals," *IEEE Trans. Commun.*, vol. 61, no. 5, pp. 1891–1901, May 2013.
[25] K. Anoh, C. Tanriover, and B. Adebisi, "On the optimization of iterative clipping and filtering for PAPR reduction in OFDM systems," *IEEE Access*, vol. 5, pp. 12004–12013, 2017.
[26] X. Liu, X. Zhang, J. Xiong, and J. Wei, "An enhanced iterative clipping and filtering method using time-domain kernel matrix for PAPR reduction in OFDM systems," *IEEE Access*, vol. 7, pp. 59466–59476, 2019.
[27] L. Wang and C. Tellambura, "A simplified clipping and filtering technique for PAR reduction in OFDM systems," *IEEE Signal Process. Lett.*, vol. 12, no. 6, pp. 453–456, 2005.
[28] I. Sohn and S. C. Kim, "Neural network based simplified clipping and filtering technique for PAPR reduction of OFDM signals," *IEEE Commun. Lett.*, vol. 19, no. 8, pp. 1438–1441, Aug. 2015.
[29] B. Tang, K. Qin, X. Zhang, and C. Chen, "A clipping-noise compression method to reduce PAPR of OFDM signals," *IEEE Commun. Lett.*, vol. 23, no. 8, pp. 1389–1392, Aug. 2019.
[30] A. Sahin, I. Guvenc, and H. Arslan, "A survey on multicarrier communications: Prototype filters, lattice structures, and implementation aspects," *IEEE Commun. Surveys Tuts.*, vol. 16, no. 3, pp. 1312–1338, 3rd Quart., 2014.
[31] Y. Medjahdi, S. Traverso, R. Gerzaguet, H. Shaïek, R. Zayani, D. Demmer, R. Zakaria, J.-B. Doré, M. B. Mabrouk, D. Le Ruyet, Y. Louët, and D. Roviras, "On the road to 5G: Comparative study of physical layer in MTC context," *IEEE Access*, vol. 5, pp. 26556–26581, 2017.
[32] H. Shaiek, R. Zayani, Y. Medjahdi, and D. Roviras, "Analytical analysis of SER for beyond 5G post-OFDM waveforms in presence of high power amplifiers," *IEEE Access*, vol. 7, pp. 29441–29452, 2019.
[33] T. Jiang, M. Guizani, H.-H. Chen, W. Xiang, and Y. Wu, "Derivation of PAPR distribution for OFDM wireless systems based on extreme value theory," *IEEE Trans. Wireless Commun.*, vol. 7, no. 4, pp. 1298–1305, Apr. 2008.
[34] H. Ochiai and H. Imai, "On the distribution of the peak-to-average power ratio in OFDM signals," *IEEE Trans. Commun.*, vol. 49, no. 2, pp. 282–289, Feb. 2001.
[35] K. Anoh, C. Tanriover, B. Adebisi, and M. Hammoudeh, "A new approach to iterative clipping and filtering PAPR reduction scheme for OFDM systems," *IEEE Access*, vol. 6, pp. 17533–17544, 2018.
[36] H. Guo and C. S. Burrus, "Wavelet transform based fast approximate Fourier transform," in *Proc. IEEE ICASSP*, vol. 3, Apr. 1997, pp. 1973–1976.
[37] S. C. Thompson, J. G. Proakis, and J. R. Zeidler, "The effectiveness of signal clipping for PAPR and total degradation reduction in OFDM systems," in *Proc. IEEE Global Telecommun. Conf.*, St. Louis, MO, USA, Nov./Dec. 2005, p. 2811.

BO TANG received the bachelor's and master's degrees in measuring and testing technologies from the University of Electronic Science and Technology of China, Chengdu, China, in 2005 and 2008, respectively, where he is currently a Lecturer with the School of Aeronautics and Astronautics. His research interests include wireless communication, radio frequency and communication testing, and signal processing.

KAIYU QIN received the master's degree in testing technology and instrumentation and the Ph.D. degree in circuits and systems from the University of Electronic Science and Technology of China, in April 1994 and March 1999, respectively. He has been teaching and researching at the University of Electronic Science and Technology of China, since 1994, and was hired as a Professor, in 2005. He is currently the Dean of Aircraft Swarm Intelligent Sensing and Cooperative Control Key Laboratory of Sichuan Province. He is a member of the China Aerospace Society Deep Space Exploration Professional Committee and the China Aeronautical Society's Near Space Professional Committee. He was awarded the title of Excellent Talent of the New Century by the Ministry of Education, China.

HAIBO MEI received the B.Sc. and M.Sc. degrees from the School of Computer Science and Engineering, University of Electronic Science and Technology of China, in 2005 and 2008, respectively, and the Ph.D. degree from the School of Electronic Engineering and Computer Science, Queen Mary University of London (QMUL), U.K., in 2012. He was a Postdoctoral Research Assistant with QMUL and a Senior Research and Development Engineer with Securus Software Ltd, U.K. He is currently a Lecturer with the University of Electronic Science and Technology of China. His research interests include resource efficiency and self-organization of wireless communications, intelligent transportation system, and mobile cloud computing.

CHANGWEI CHEN received the master's degree in measuring and testing technologies and instruments engineering from the University of Electronic Science and Technology. He is currently with the University of Electronic Science and Technology. His current research interests include amplifier linearization and wideband matching circuits, microwave/millimeter wave circuits, radio transceivers and RF front ends, circuits and systems, electromagnetic theory, and signal processing.